



## Broadband and ultra-long offset *mCSEM* – A recipe for complex subsalt imaging

Andrea Zerilli, Tiziano Labruzzo and Adriano Aguiar Marçal, Schlumberger BRGC, Marco Polo Buonora, João Lucas Crepaldi and Paulo T. L. Menezes, Petrobras E&P/GEOF/MNS

Copyright 2015, SBGf - Sociedade Brasileira de Geofísica

This paper was prepared for presentation during the 14<sup>th</sup> International Congress of the Brazilian Geophysical Society held in Rio de Janeiro, Brazil, August 3-6, 2015.

Contents of this paper were reviewed by the Technical Committee of the 14<sup>th</sup> International Congress of the Brazilian Geophysical Society and do not necessarily represent any position of the SBGf, its officers or members. Electronic reproduction or storage of any part of this paper for commercial purposes without the written consent of the Brazilian Geophysical Society is prohibited.

### Abstract

We present the results of a demonstration research multi-component, ultra-long offset, broadband marine Controlled Source Electromagnetic (*mCSEM*) survey that was carried out over selected ultra-deep water area of the Espírito Santo Basin (offshore Brazil), where the presence of allochthonous salt structures makes around-salt and subsalt seismic depth imaging extremely challenging.

We explain the workflows that we developed to combine and exploit the additional information that ultra-long offset, broadband *mCSEM* may provide to define and constrain ultra-deep water complex allochthonous salt geometries and salt, around-salt, subsalt multi-properties distribution such as the ones encountered in the Espírito Santo Basin and thus improve the seismic imaging through an enhanced velocity model and novel velocity model building.

We show that the reconstructed resistivities, velocities and shapes of regions of interest are consistent with both the *EM* and the seismic data and that considerable improvement in resolution and speed is achieved compared to the current state-of-the-art.

The results presented falsify the allochthonous base of salt (BOS) interpreted from NAZ seismic and hence providing an additional data set, that can be used as a cost-effective solution for integrated analysis, input for Reverse Time Migration (RTM) or as a starting point for Full Waveform Inversion (FWI).

### Introduction

Salt basins, especially tertiary basins with mobilized salt, are notoriously difficult places to explore because of the traditionally poor subsurface images typically obtained around and below salt. The high-velocity and laterally varying overburden also introduces uncertainties in the velocity estimation needed for accurate depth imaging.

While most of the progress has come through new seismic acquisition techniques, such as wide-azimuth surveys (WAZ), rich-azimuth surveys (RAZ), full-azimuth surveys (FAZ) and a resulting alphabet soup of specialized wide azimuth acquisitions, imaging through the incorporation of better physics has come in the form of reverse time migration (RTM) with full anisotropy.

However, not every subsalt problem has been solved, and many challenges remain.

In areas where the salt structures are extremely complex, the seismic signal to noise ratio (SNR) may still be limited and therefore complicate the estimation of the velocity field variations that could be used to correctly migrate the seismic data and recover a good image suitable for prospect generation.

Additional earth model constraints or enhancements to the seismic-derived velocity model might significantly improve depth imaging through integration of multiple geophysical domains such as deep reading electromagnetics (*EM*) and potential fields. Salt bodies generally have a higher seismic velocity than the surrounding sediments, and they also have a higher resistivity than these sediments. The higher velocity can diffract seismic raypaths and reduce the propagated energy that is transmitted to the sediments below. However, the higher salt resistivity deflects telluric currents, allowing *EM* to detect and map the salt. In addition, gravity and full tensor gradient (FTG) data are also sensitive to the presence of salt, being these much lighter in terms of density if compared to the surrounding sediments.

The purpose is to develop a cost-effective alternative to very expensive WAZ or FAZ seismic acquisition and advanced depth migration facilitating the task of velocity model building through implementation of an integrated inversion of different geophysical domains where the seismic imaging conditions are taken and built in the integrated inversion scheme. This ensures that the resulting velocity models are consistent with the requirements of improving the seismic image quality when migrated to depth.

If the existence of resistivity-velocity trends can be assumed, deep reading *EM* may provide through integrated inversion an important contribution to the velocity determination and velocity model building problems at considerably lower costs.

The conductive seawater in the ocean has an attenuating effect on the incident Magnetotelluric (*MT*) source fields and acts as a low-pass filter. Fields with skin depths much less than the ocean depth will experience severe attenuation, limiting the highest frequency *MT* fields observable on the seafloor. To overcome this severe attenuation, Controlled-source Electromagnetics (*mCSEM*) has been applied which utilizes an artificial grounded dipole as a signal source. *CSEM* serves as a 'near-surface' supplement to *MT* providing the higher frequency content necessary for a more robust inversion/interpretation of the data. Broadband *mCSEM* gives further possibility to improve resolution and reduce interpretation ambiguities [Vöge et al. 2010; Zerilli et al., 2014] when *MT* data fall far short the high frequency coverage needed to provide rigorous constraints on the

'deep' structure information contained in the lower frequency data and are also highly distorted by seafloor bathymetry and coastline on local and regional scale, making essential the inclusion of accurate bathymetric modelling and inversion for the correct interpretation of seafloor geology including the targeted salt body(ies).

### The Espirito Santo broadband *mCSEM* acquisition

The Espirito Santo broadband *CSEM* acquisition was carried out using acquisition parameters determined through extensive sensitivity analysis where for each frequency and offsets, the effects of the suprasalt, BOS, subsalt and around salt sediments were modelled in terms of amplitude and phase changes in the *EM* components.

A total of 434 km of *mCSEM* towlines were towed twice over the same 157 receivers deployed at water depths ranging from -1730 to -2280 meters. The base frequency was 0.25 Hz for towlines *01Tx001*, *02Tx001*, *03Tx001* and 0.0625 Hz for towlines *01Tx002*, *02Tx002*, *03Tx002*, (Figure 1). All receivers measured both the horizontal electric and horizontal magnetic fields in two orthogonal directions. Five harmonics (0.75, 1.25, 2.25, 2.75, 3.25 Hz) were computed from the 0.25 Hz base frequency and four harmonics (0.1875, 0.3125, 0.5625, 0.8125 Hz) were computed from the 0.0625 Hz base frequency.

The increased number of frequencies determined from the sensitivity analysis made the data richer in potential bandwidth and resolution for enhanced complex overburden, 'deep' subsalt and around salt imaging. The recorded *mCSEM* data were of very good quality and achieved usable offsets exceeding 25 km for the lowest frequencies. An extended deployment period allowed for the acquisition of collocated *MT* data.

### Integrated interpretation workflow

Multi-dimensional inversion of *geophysical* data to obtain multi-properties-depth images is a non-unique process and, if begun with a non-robust initial model, creates models characterized by a high degree of non-uniqueness. Smoothness and/or flatness constraints are able to extract large scale geological structures and tend to produce smoothed models, therefore sharp contrasts in the earth such as salt flanks and salt base boundaries are not easily identified and smeared out providing sometimes an 'answer looking for questions'.

To overcome the limitation of smoothness regularization, the inversion approach utilized in this work begins with a 'smoothly' regularized anisotropic inversion with starting models in which the 'property mesh' is constructed from seismic interpretation in depth and properties, derived from the well log database and reconnaissance modeling, are mapped into the seismically-derived mesh, followed by a constrained 'structure'-based approach in which locations, shapes, properties of the interpreted 'allochthonous' salt bodies are further constrained.

### The Espirito Santo broadband *mCSEM* data inversion

The *mCSEM* data inversion was based on an irregular mesh model representation of the resistivity structure (Figure 2) where a finite difference solution is used to solve the Maxwell's equations in the frequency domain [Mackie et al., 2007].

The fundamental transmission frequencies (0.25 and 0.0625 Hz) plus all harmonics for each towline (0.75, 1.25, 2.25, 2.75, 3.25 Hz) and (0.1875, 0.3125, 0.5625, 0.8125 Hz) were used in the *mCSEM* inversion for the *E<sub>x</sub>* and *H<sub>y</sub>* measured field components.

The 3D computational mesh (Figure 2) was generated from such specified parameters as: receiver and source locations, resistivities (and resistivity contrasts) of the model.

The 3D 'image'-based inversion phase displayed along the *L<sub>QQ</sub>* line, beginning with an initial model based on: a) seismic interpretation; b) 'allochthonous' salt bodies 'smoothly' constrained; c) resistivity distribution provided from well log database and reconnaissance modelling (Figure 3), shows sensitivity to strong resistors evident in the vertical resistivity cross-section (Figure 4). We see the appearance of vertical conductors bounding the massive salt bodies (e.g. *B<sub>QQ</sub>*) in the vertical resistivity inversion. These vertical conductors could be explained by a combination of phenomena related to possible salt dissolution, which decreases the overall bulk resistivity of rock formations around the massive salt bodies, or by a structural setup of layered evaporites (believed to be highly anisotropic) when they sub-vertically onlap onto the massive salt bodies. If present and sub-vertically stratified, these layered evaporites anisotropy becomes HTI (horizontal transverse isotropy). The above considerations would lead to the conclusion that more complex electrical anisotropy models such as tilted transverse isotropy (TTI) involving the off-diagonal components of the conductivity tensor should be invoked to explain the propagation of *CSEM* fields in structured and anisotropic complex salt geology.

These resistors with averaged regularized vertical resistivities > 4000 Ohm.m are recovered at approximate depths of -2700 to -2900; -3400 to -3700 (top) and -3900 to -4200; -4400 to -4800 (BOS) b.m.s.l. and their lateral extent imaged. These resistors are related to the 'allochthonous' salt bodies detached from/rooted to the deep 'autochthonous' salt.

While NAZ seismic leaves large uncertainties in the interpretation of the shape, size and base of the salt bodies, the *mCSEM* 'image'-based inversion delivers a clearer image of the salt structures and their base.

The starting model for the 'structure'-based inversion was then constructed using the resistivity distribution recovered by the 'image'-based inversion introducing boundary-preserving constrained inversion to preserve the sharp contrast at the 'allochthonous' BOS boundaries and give better estimation of the salt 'geobodies' resistivities. The objective of the 'structure'-based inversion is to give a complete and geologically reasonable definition of regions-of-interest (ROI) by resolving their resistivities, location and shape. Only the data that contribute to the image in a ROI are used in the process. The Regularization breaks (or tear surfaces) approach [Mackie et al., 2007], [Farquharson, 2008] was

used. This scheme forces the inversion not to smooth across a certain discontinuity. This is relevant if a significant resistivity change is expected at that interface (BOS, etc.) and if reliable 'image'-based interpretation is available.

Figures 5 and 6 show that the 'structure'-based inversion results in a significantly improved image giving better estimation of resistivities in the allochthonous salt bodies leading to an updated salt interpretation and insight into the salt composition and degrees of heterogeneity, separating BOS boundaries from 'uncertain regions' where the salt (e.g. salt body labelled B<sub>QQ</sub>) and sediment boundaries were not properly discriminated by the 'image'-based inversion.

*More importantly, Figures 5 and 6 clearly show that the base of salt was determined to be about 300 to 700 meters shallower than that interpreted from the NAZ seismic.*

The allochthonous salt body B<sub>QQ</sub> steeply dipping flank walls and an Early Tertiary minibasin are also much better delineated increasing the resolution and precision thus reducing the ambiguity in interpretation and for the prospectivity of the basin. Incorporation of the obtained resistivity image into the velocity model-building workflow will attain subsalt images suitable for hydrocarbon exploration beneath and around such complexly shaped salt bodies.

Figures 7 and 8 show normalized amplitude pseudo-sections at 0.0625 and 0.25 Hz to final inversion model, respectively. These normalized pseudo-sections show that the data are well fit, considering the geological complexity, by the 'structure'-based inversion.

## Conclusions

We have shown how ultra-long offset, broadband *mCSEM* extending to frequencies as low as 16 seconds provides a powerful tool for imaging complex overburden and deeper structures such as the Espirito Santo complex BOS with higher multiscale resolution, data coverage and redundancy.

We also presented the potential of a new integrated seismic-*EM* inversion in addressing the major critical steps in subsalt and around salt imaging: estimation of resistivities/velocities above the salt, definition of salt geometry and subsalt resistivity/velocity update.

The integrated inversion reconstructs the properties and shapes within regions-of-interest (ROI) using an 'image'-based inversion approach followed by a 'structure'-based inversion algorithm where the ROI are parameterized using both surfaces and bodies for localized targeting and rapid inversion. This workflow preserves the velocity and resistivity structure already arrived at, enabling the integration of geology in the geophysical process. The 'structure'-based inversion is capable of quantitatively reconstruct the velocities, resistivities of regions-of-interest and placed them accurately both laterally and in depth guided not only by the data but also by geological consistency preventing smoothing across them, allowing for: faster velocities and resistivities model building, targeting salt bodies, focusing on geobodies.

We have shown that the reconstructed properties and shapes of the Espirito Santo allochthonous salt bodies are consistent with both the *EM* and the seismic data and that considerable improvement in resolution and speed is achieved compared to the current state-of-the-art.

Our example along the L<sub>QQ</sub> line shows that this methodology falsify the allochthonous salt BOS interpreted from NAZ seismic and hence providing an excellent additional data set, that may be used for integrated analysis, input for RTM or as a starting point for FWI.

While we believe that the broadband *mCSEM* coupled with the integrated interpretation yield great improvement in around-salt and subsalt model building, we expect that the real value will come from the use of these models in RTM and FWI workflows.

## Acknowledgments

We are thankful for the help from the management in both Petrobras and Schlumberger. We are extremely grateful for the contribution of Gustavo Basta Dos Santos Silva and Rafael Correia Freitas of Petrobras EXP/IABCS/PN, for their great knowledge of the Espirito Santo seismic and geology. Mikhail Zaslavsky of Schlumberger-SDR helped this project tremendously by extending our 3D code functionality.

## References

- Farquharson, C.G., **2008**, Constructing piecewise-constant models in multidimensional minimum-structure inversions: *Geophysics*, 73, no. 1, K1–K9.
- Mackie, R. L., M. D. Watts, and W. Rodi, **2007**, Joint 3D inversion of marine CSEM and MT data, 77th SEG Annual International Meeting, San Antonio, TX, Expanded Abstract, 574-578.
- Vöge, M., A. A. Pfaffhuber, K. Hokstad, and B. Fotland, **2010**, A Broadband Marine CSEM Demonstration Survey to Map the Uranus Salt Structure: 72nd EAGE Conference & Exhibition incorporating SPE EUROPEC 2010, Barcelona, Spain, 14-17 June 2010.
- Zerilli, A., Labruzzo, T., Zanzi, M., Buonora, M.P., Crepaldi, J.L., Menezes, P.T.L., **2014**, Broadband marine CSEM: New benefits for subsalt and around salt exploration, Society of Exploration Geophysicist 84rd Annual Meeting and Exposition, 26-31 October, Denver, Colorado, 750-754.

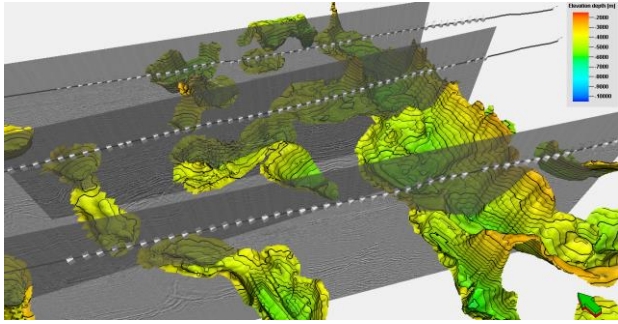


Figure 1. Broadband *mCSEM* acquisition location with respect to the area's Allochthonous salt distribution (BOS from NAZ seismic interpretation).

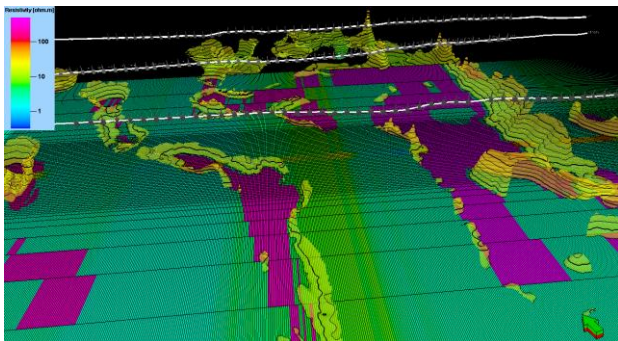


Figure 2. Espirito Santo allochthonous salt top from interpreted NAZ seismic mapped on the inversion domain grid. Resistivity-depth slice extracted at -4200 meters b.m.s.l.

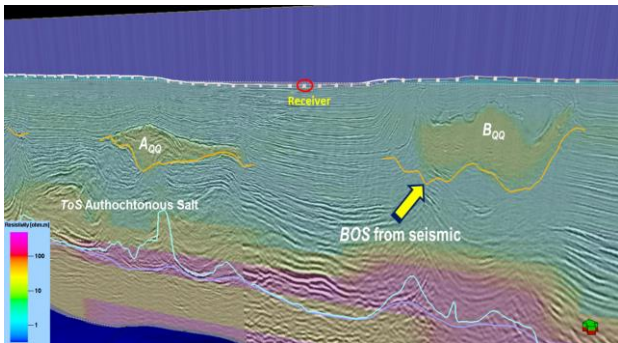


Figure 3. Initial model cross-section for 3D 'image'-based inversion along L\_QL. Vertical resistivity. Initial model based on: a) seismic interpretation; b) well log database c) background reconstruction from reconnaissance modelling. 'Allochthonous' salt bodies 'smoothly' constrained. Orange lines correspond to Base of Allochthonous salt from NAZ seismic interpretation.

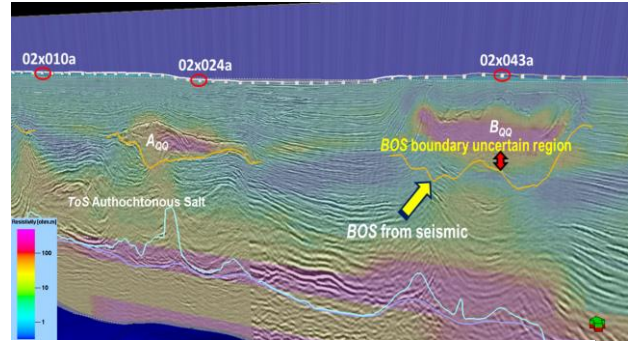


Figure 4. Vertical resistivity cross-section from 3D 'image'-based inversion along L\_QL. Orange lines correspond to Base of Allochthonous salt from NAZ seismic interpretation.

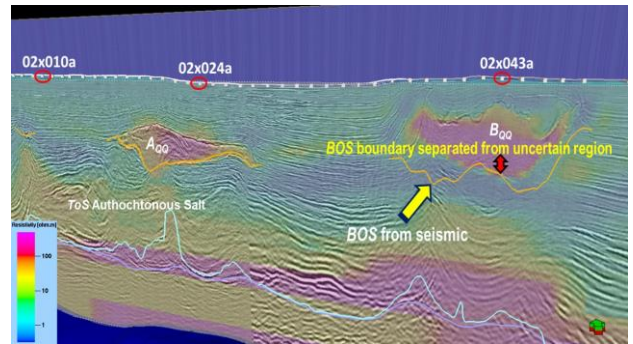


Figure 5. Vertical resistivity cross-section from 3D 'structure'-based inversion along L\_QL. BOS, width and magnitude at the center of the 'allochthonous' salt bodies are now resolved more accurately. BOS separated from uncertain regions where the salt and sediment boundaries were not properly discriminated by the 'image'-based inversion. Uncertain regions are here defined as localized 'blurred edges' that are generally wider than the 'sharp ones' based on the interpreter's visual inspection. Orange lines correspond to Base of Allochthonous salt from NAZ seismic interpretation.

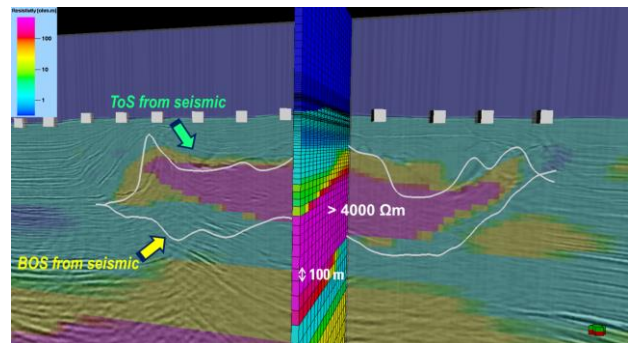


Figure 6. Vertical resistivity cross-sections from 3D 'structure'-based inversion along (W-E) and crossing (S-N) L\_QL. BOS, width and magnitude at the center of the 'allochthonous' salt bodies are now resolved more accurately. BOS separated from uncertain regions where the salt and sediment boundaries are not properly discriminated by the 'image'-based inversion. 3D inversion results falsify the allochthonous B<sub>00</sub> BOS interpreted from NAZ seismic. Figure clearly shows that B<sub>00</sub> BOS is determined to be about 300 to 700 meters 'shallower' than that interpreted from seismic.

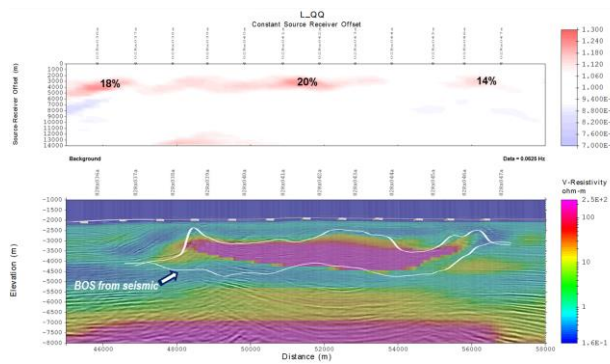


Figure 7. Vertical resistivity cross-section from 3D 'structure'-based inversion along L\_QQ. BOS of  $B_{00}$  salt body between receivers 02Rx038a and 02Rx046a. The upper part of the figure shows normalized amplitude pseudo-section to final inversion model at 0.0625 Hz. This normalized pseudo-section shows that the data are well fit, considering the geological complexity, by the 'structure'-based inversion. White lines correspond to Top and Base of Allochthonous salt from NAZ seismic interpretation.

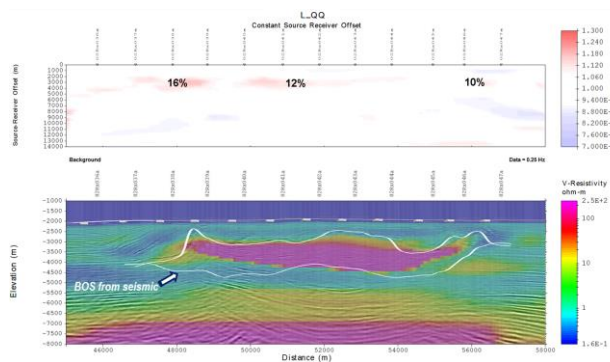


Figure 8. Vertical resistivity cross-section from 3D 'structure'-based inversion along L\_QQ. BOS of  $B_{00}$  salt body between receivers 02Rx038a and 02Rx046a. The upper part of the figure shows normalized amplitude pseudo-section to final inversion model at 0.25 Hz. This normalized pseudo-section shows that the data are well fit, considering the geological complexity, by the 'structure'-based inversion.